9542 *Biochemistry* **2010,** *49,* 9542–9550
DOI: 10.1021/bi101420w

BIOCHEMISTRY
including biophysical chemistry & molecular biology
Article

Steady-State Kinetic Mechanism and Reductive Half-Reaction of D-Arginine Dehydrogenase from *Pseudomonas aeruginosa*†

Hongling Yuan,‡ Guoxing Fu,§ Phillip T. Brooks,‡ Irene Weber,‡,§,∥ and Giovanni Gadda*,‡,§,∥

‡*Departments of Chemistry,* §*Biology, and* ∥*The Center for Biotechnology and Drug Design, Georgia State University, Atlanta, Georgia 30302-4098, United States*

Received September 2, 2010; Revised Manuscript Received October 8, 2010

ABSTRACT: D-Arginine dehydrogenase from *Pseudomonas aeruginosa* catalyzes the oxidation of D-arginine to iminoarginine, which is hydrolyzed in solution to ketoarginine and ammonia. In the present study, we have genetically engineered an untagged form of the enzyme that was purified to high levels and characterized in its kinetic properties. The enzyme is a true dehydrogenase that does not react with molecular oxygen. Steady-state kinetic studies with D-arginine or D-histidine as substrate and PMS as the electron acceptor established a ping-pong bi-bi kinetic mechanism. With the fast substrate D-arginine a dead-end complex of the reduced enzyme and the substrate occurs at high concentrations of D-arginine yielding substrate inhibition, while the overall turnover is partially limited by the release of the iminoarginine product. With the slow substrate D-histidine the initial Michaelis complex undergoes an isomerization involving multiple conformations that are not all equally catalytically competent for the subsequent oxidation reaction, while the overall turnover is at least partially limited by flavin reduction. The kinetic data are interpreted in view of the high-resolution crystal structures of the iminoarginine− and iminohistidine−enzyme complexes.

D-Arginine dehydrogenase is a novel flavin-dependent enzyme with FAD as a cofactor (*1*). It was recently isolated from *Pseudomonas aeruginosa*, a Gram-negative soil bacterium that is well-known to be an important opportunistic human pathogen. The enzyme from *P. aeruginosa* has been cloned and expressed in *Escherichia coli* (*2*). It catalyzes the oxidation of D-arginine to iminoarginine, which is nonenzymatically hydrolyzed to α-keto-arginine and ammonia, as illustrated in Scheme 1 (*2*−*4*). Coupled with an anabolic NAD(P)H-dependent L-arginine dehydrogenase, the products of the D-arginine dehydrogenase oxidation of D-arginine, α-ketoarginine and ammonia, are converted into L-arginine (*1*). The proposed physiological function of D-arginine dehydrogenase in *Pseudomonas* is to contribute the first stage in a two-enzyme-coupled system to racemize D-arginine in the D- to L-arginine conversion (*1*).

The biochemistry of D-amino acid catabolism has been poorly studied in comparison to that of L-amino acids. In general, D-amino acids can be metabolized after conversion into the L-enantiomers by racemase (*5*). Alternatively, D-amino acids can be utilized by D-amino acid oxidase, which is an FAD-dependent enzyme and plays an important role in microbial metabolism (*6*). D-Amino acid oxidase was first studied by Krebs in 1935 (*7*) and is now well characterized. The enzyme has FAD noncovalently bound to the polypeptide and exhibits optimal activity toward neutral D-isomers of amino acids and lower efficiency toward basic ones (*8*). The reduced FAD is then reoxidized by molecular oxygen to yield hydrogen peroxide (*8*).

D-Arginine dehydrogenase is characterized by broad substrate specificity, being able to oxidize D-amino acids of various size and polarity (*9*). All naturally occurring D-amino acids except for D-glutamate, D-aspartate, and glycine are oxidized by the enzyme, with the best substrate, D-arginine, displaying the highest k_{cat}/K_m with a value of 3×10^6 M^{-1} s^{-1} (*9*). D-Arginine dehydrogenase was first described in 1988 by Hass et al. (*2*). Recently, the *dauA* gene encoding for D-arginine dehydrogenase was cloned and used to express a His-tagged version of the enzyme that was characterized crystallographically at high resolutions (i.e., ≤1.3 Å) in complex with either iminoarginine or iminohistidine (*1*, *9*). The physiological electron acceptor of the enzyme has not been identified yet (*1*).

Scheme 1: Oxidation of D-Arginine by D-Arginine Dehydrogenase

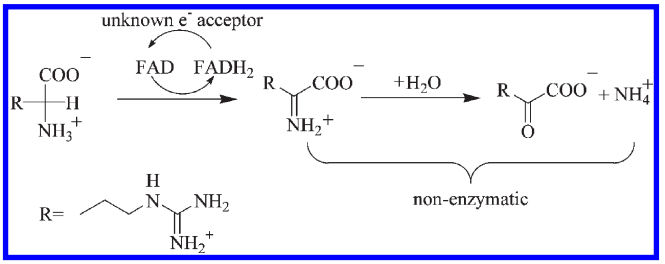

In the present study, we have genetically engineered an untagged form of D-arginine dehydrogenase, purified it to high levels, and investigated its steady-state kinetic mechanism and reductive half-reaction with the physiological substrate D-arginine and with D-histidine. The kinetic data presented are interpreted in view of the high-resolution structures of D-arginine dehydrogenase reported recently (*1*, *9*).

EXPERIMENTAL PROCEDURES

Materials. The plasmid pCR3 harboring the *dauA* gene encoding for D-arginine dehydrogenase was a gift from Prof. Chung-Dar Lu at Georgia State University. *E. coli* strain

†This work was supported in part by grants from NSF-CAREER MCB-0545712 (G.G.) and Georgia State University Molecular Basis of Disease Fellowship (G.F.).

*Address correspondence to this author at the Department of Chemistry, Georgia State University. Phone: (404) 413-5537. Fax: (404) 413-5505. E-mail: ggadda@gsu.edu.

 Published on Web 10/08/2010

Rosetta(DE3)pLysS was from Novagen (Madison, WI). *Nde*I, *Bam*HI, alkaline phosphatase, T4 DNA ligase, dNTPs,[1] BSA, lambda DNA/*Eco*RI + *Hin*dIII markers, and $MgCl_2$ were purchased from Promega (Madison, WI); cloned *Pfu* DNA polymerase was from Stratagene (La Jolla, CA); QIAprep and QIAquick purification kits were from Qiagen (Valencia, CA); Luria−Bertani agar, Luria−Bertani broth, chloramphenicol, IPTG, lysozyme, sodium hydrosulfite (dithionite), D-arginine, phenazine methosulfate (PMS), and PMSF were obtained from Sigma-Aldrich (St. Louis, MO). Ampicillin, agarose, and electrophoresis-grade agar were purchased from ICN Biomedicals (Aurora, OH). Oligonucleotides were from Sigma Genosys (The Woodlands, TX). D-Histidine was from Alfa Aesar (Ward Hill, MA). All of the other reagents were of the highest purity commercially available.

Plasmid Construction. Plasmid pCR3 harboring the *dauA* gene encoding for D-arginine dehydrogenase (*1*) was employed as template to construct a recombinant plasmid for the expression of untagged enzyme using standard PCR amplification methods. Forward and reverse oligonucleotide primers were designed incorporating *Nde*I and *Bam*HI as the 5′ and 3′ cloning sites, respectively. The PCR product was then ligated into the expression vector pET20b(+) cleaved with the same restriction enzymes to ensure directional cloning to remove the N-terminal His tag. The resulting plasmid pET/*PA3863* was confirmed by sequencing and transformed into *E. coli* strain DH5α.

Gene Expression and Enzyme Purification. Permanent frozen stocks of *E. coli* cells Rosetta(DE3)pLysS harboring the plasmid pET/*PA3863* were used to inoculate 50 mL of Luria−Bertani broth medium containing 50 μg/mL ampicillin and 34 μg/mL chloramphenicol, and cultures were grown at 37 °C for 16 h to be used as a preculture. The starting precultures (48 mL) were used to inoculate 7.5 L of Luria−Bertani broth medium containing 50 μg/mL ampicillin and 34 μg/mL chloramphenicol. When the cultures reached optical densities of ∼0.6 at 600 nm, the temperature was lowered to 18 °C, and IPTG was added to a final concentration of 0.1 mM. After 18 h the cells were harvested by centrifugation at 20000*g* for 20 min at 4 °C.

All purification steps were carried out at 4 °C. The wet cell paste was suspended in 0.1 mM PMSF, 0.2 mg/mL lysozyme, 1 mM EDTA, 10% glycerol, and 20 mM Tris-HCl, pH 8.0, in a ratio of 1 g of wet cell paste to 4 mL of lysis buffer. The suspended cells were then allowed to incubate with stirring for 30 min on ice with 20 μg/mL RNase and 50 μg/mL DNase in the presence of 10 mM $MgCl_2$. The resulting slurry was sonicated five times for 5 min, with 2 min intervals, before removing the cell debris by centrifugation at 20000*g* for 20 min. Solid ammonium sulfate was slowly added to the cell free extract to achieve 30% saturation. After incubating for 30 min on ice, the insoluble fraction was removed by centrifugation and discarded. The supernatant was brought up to 65% ammonium sulfate saturation, and the pellet fraction was collected by centrifugation after 30 min of stirring. The resulting pellet was suspended in 20 mM Tris-HCl, pH 8.0, and 10% glycerol and dialyzed over a period of 18 h with four buffer changes. After dialysis, the precipitated proteins were removed by centrifugation at 20000*g* for 20 min, and the supernatant was loaded directly onto a DEAE-Sepharose Fast Flow column (3 × 28 cm), equilibrated with 20 mM Tris-HCl, pH 8.0, and 10% glycerol. The column was eluted with 2 volumes of the same buffer, followed by a linear gradient from 0 to 0.5 M NaCl over 1 L. The fractions with the highest purity as judged by enzymatic activity and UV−visible absorbance spectroscopy were pooled together and concentrated with the addition of 65% ammonium sulfate saturation followed by centrifugation. After centrifugation, the resulting pellet was suspended in 20 mM Tris-HCl, pH 8.7, and 10% glycerol and dialyzed against four changes of the same buffer. After removal of the precipitated protein by centrifugation, the enzyme was stored at −20 °C.

Enzyme Assay. The concentration of D-arginine dehydrogenase was determined with the method of Bradford (*10*) by using the Bio-Rad protein assay kit with BSA as standard. The enzymatic activity of D-arginine dehydrogenase was measured by monitoring the initial rate of oxygen consumption with a computer-interfaced Oxy-32 oxygen-monitoring system (Hansatech Instrument) at 25 °C in which PMS (1 mM) was used as the primary electron acceptor, and the enzymatically reduced PMS was spontaneously reoxidized by molecular oxygen. The reaction was started with the addition of D-arginine dehydrogenase to 1 mL reaction mixture, with the final concentration of 9.9 nM enzyme and 20 mM D-arginine. One unit of enzymatic activity corresponds to the consumption of 1 μmol of oxygen/min.

First-order rate constants for flavin reduction were determined at varying concentrations of D-arginine (0.1−0.5 mM) or D-histidine (2.5−100 mM) in 20 mM Tris-HCl, pH 8.7, using a stopped-flow spectrophotometer thermostated at 25 °C. Equal volumes of the enzyme and D-arginine or D-histidine were mixed anaerobically in the stopped-flow spectrophotometer following established procedures (*11*) yielding a final enzyme concentration of ∼10 μM. The stopped-flow traces were not changed when the experiment was carried out aerobically.

The determination of the steady-state kinetic parameters was carried at varying concentrations of D-arginine (0.02−2 mM) or D-histidine (1−70 mM) and PMS (0.005−0.5 mM), in 20 mM Tris-HCl, pH 8.7, 25 °C. The reaction mixture (1 mL) was first equilibrated with the substrates at the desired concentrations before the reaction was started with the addition of the enzyme to a final concentration of ∼0.01 μM. Enzyme assays were conducted in 20 mM Tris-HCl, pH 8.7. Initial rates of reaction were expressed per molar content of enzyme-bound flavin. Solvent viscosity effects on steady-state kinetic parameters were measured in 20 mM Tris-HCl, pH 8.7, 25 °C, using glycerol as viscosigen. The values for the relative viscosities of glycerol-containing solutions were taken from Weast (*12*) and adjusted for 25 °C.

Data Analysis. Data analysis was carried out by using KaleidaGraph software (Synergy Software, Reading, PA), Enzfitter software (Biosoft, Cambridge, U.K.), or the Kinetic Studio Software Suite (Hi-Tech Scientific, Bradford on Avon, U.K.). Stopped-flow traces were fit to eq 1, which describes a single exponential process, where k_{obs} represents the observed first-order rate constant for flavin reduction at any given concentration of substrate, t is time, A is the absorbance at 446 nm at any given time, B is the amplitude of the absorbance change, and C is the absorbance at infinite time. Kinetic parameters for the reductive half-reactions were determined by using eq 2, where k_{obs} is the observed first-order rate constant for the reduction of the enzyme-bound flavin at any given concentration of substrate (S), k_{red} is the limiting first-order rate constant for flavin reduction at saturating concentrations of substrate, and $^{app}K_d$

[1]Abbreviations: dNTPs, deoxynucleoside triphosphates; IPTG, isopropyl β-D-thiogalactopyranoside; PMS, phenazine methosulfate; PMSF, phenylmethanesulfonyl fluoride; DEAE, diethylaminoethyl.

Table 1: Purification of Untagged *P. aeruginosa* D-Arginine Dehydrogenase Expressed in *E. coli* Rosetta(DE3)pLysS[a]

step	total protein (mg)	total activity (μmol of O_2 min^{-1})	specific activity (μmol of O_2 min^{-1} mg^{-1})	yield (%)
cell-free extract	5600	91200	16	100
30−65% saturation of $(NH_4)_2SO_4$	4700	100000	21	110
DEAE-Sepharose	900	43000	48	47

[a]Enzymatic activity was measured with 20 mM D-arginine and 1 mM PMS as substrates in air-saturated 20 mM Tris-HCl, pH 8.7 and 25 °C.

is the apparent dissociation constant for binding of the substrate to the enzyme.

$$A = B\exp(-k_{obs}t) + C \quad (1)$$

$$k_{obs} = \frac{k_{red}S}{^{app}K_d + S} \quad (2)$$

The steady-state kinetic parameters at varying concentrations of both D-arginine and PMS were determined by fitting the initial rate data to eq 3, which describes a ping-pong mechanism with substrate inhibition (*13*). Data with D-histidine were fit with eq 4, which describes a ping-pong steady-state kinetic mechanism. In these equations, *e* represents the concentration of enzyme, k_{cat} is the turnover number of the enzyme at saturating concentrations of both the amino acid and PMS, K_a and K_b represent the Michaelis constants for the amino acid (*A*) and PMS (*B*), respectively, and $K_{i\text{-}A}$ is the substrate inhibition constants for D-arginine.

$$\frac{v}{e} = \frac{k_{cat}ABK_{i\text{-}A}}{K_aBK_{i\text{-}A} + K_bAK_{i\text{-}A} + ABK_{i\text{-}A} + K_bA^2} \quad (3)$$

$$\frac{v}{e} = \frac{k_{cat}AB}{K_aB + K_bA + AB} \quad (4)$$

The effects of solvent viscosity on the k_{cat} and k_{cat}/K_{Arg} values were fit to eq 5; those on the k_{cat}/K_{His} values were fit to eq 6. In these equations $(k)_0$ and $(k)_\eta$ are the kinetic parameters of interest in the absence and presence of the viscosigen, *S* is the degree of viscosity dependence, η_{rel} is the relative viscosity of the aqueous buffered solution, and Y_H is the limiting value of the steady-state kinetic parameter of interest at high concentration viscosigen.

$$\frac{(k)_0}{(k)_\eta} = S(\eta_{rel} - 1) + 1 \quad (5)$$

$$\frac{(k)_0}{(k)_\eta} = \frac{1}{1 + \frac{Y_H(\eta_{rel} - 1)}{(\eta_{rel} - 1) + S}} \quad (6)$$

RESULTS

Expression and Purification of Untagged Enzyme. Recombinant D-arginine dehydrogenase was expressed in *E. coli* strain Rosetta(DE3)pLysS and purified via 30−65% ammonium sulfate precipitation and anionic-exchange chromatography at pH 8.0 in the presence of 10% glycerol. The purity of the enzyme was confirmed by SDS−PAGE analysis. The UV−visible absorbance spectrum of the purified enzyme showed bands at 365 and 446 nm (data not shown), consistent with the presence of oxidized flavin bound to the enzyme. Table 1 summarizes the purification procedure.

Oxygen Reactivity. The reactivity of D-arginine dehydrogenase with molecular oxygen was investigated by monitoring oxygen consumption over time upon mixing 0.3 μM enzyme with 0.5 mM D-arginine in a Clark-type oxygen electrode at pH 8.7 and 25 °C. As shown in Figure 1, in the absence of any organic electron acceptor there was no detectable consumption of oxygen. In contrast, upon addition of 1 mM PMS there was a rapid depletion of oxygen in the enzyme reaction mixture (i.e., with an estimated v_o/e value of ~800 s^{-1} with 0.5 mM D-arginine). Similar results were obtained with D-lysine, D-histidine, D-serine, D-threonine, D-tyrosine, D-asparagine, D-glutamine, D-alanine, D-valine, D-leucine, D-isoleucine, D-phenylalanine, D-methionine, D-proline, and D-tryptophan as a substrate (data not shown). These data unequivocally establish the enzyme as a true dehydrogenase with very poor, if any, reactivity of the reduced flavin with molecular oxygen.

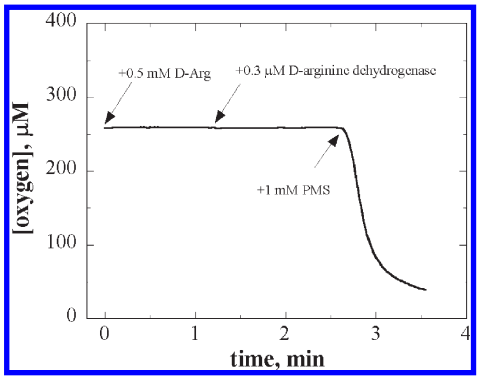

FIGURE 1: Lack of reactivity of D-arginine dehydrogenase with molecular oxygen. The assay mixture contained 20 mM Tris-HCl, pH 8.7, and 0.5 mM D-arginine, at 25 °C. After monitoring the background for 1 min, 0.3 μM D-arginine dehydrogenase was added to enzyme reaction mixture, and the oxygen trace was monitored. Later (1.5 min), 1 mM PMS was added, and the rate of the enzymatic reaction was monitored.

Time-Resolved Flavin Reduction with D-Arginine or D-Histidine. The reductive half-reactions in which the enzyme-bound flavin is reduced with D-arginine or D-histidine were investigated in a stopped-flow spectrophotometer at pH 8.7 and 25 °C. With D-arginine under conditions of pseudo first order (i.e., 10 μM enzyme and ≥50 μM D-arginine after mixing), ~70% of the decrease in absorbance at 446 nm occurred within the dead time of the instrument (i.e., 2.2 ms). From the final part of the reduction process that could be monitored, similar k_{obs} values ~700 s^{-1} were determined with 50, 100, or 500 μM D-arginine. These data did not allow for an accurate determination of the kinetic parameters k_{red} and K_d but are at least consistent with a fast process of flavin reduction ($k_{red} \geq 700\ s^{-1}$) and suggest a K_d value for D-arginine significantly lower than 50 μM. With D-histidine as a substrate, the decrease in absorbance at 446 nm associated with the reduction of the enzyme-bound flavin was monophasic at all the concentrations of substrate and fit best to a single exponential process (Figure 2A). The observed rate constants were hyperbolically dependent on the concentration of D-histidine (Figure 2B), allowing for the determination of the rate

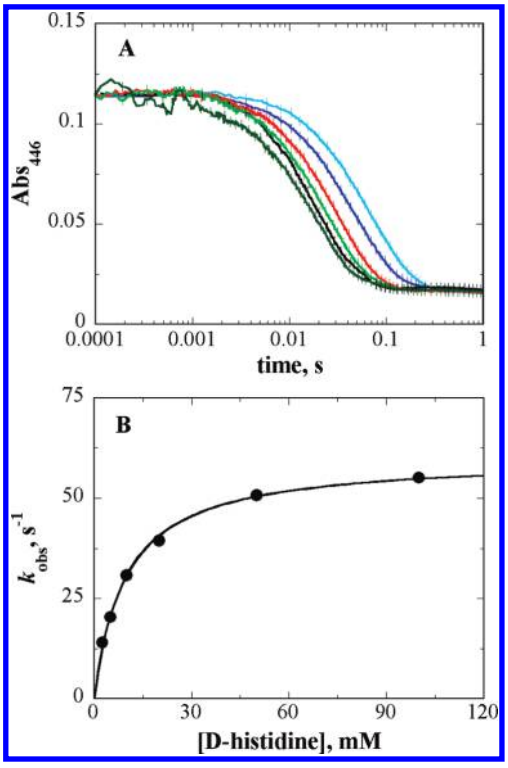

FIGURE 2: Anaerobic reduction of the D-arginine dehydrogenase with D-histidine as a substrate in 20 mM Tris-HCl, pH 8.7 and 25 °C. Panel A shows the reduction traces with 2.5 mM (cyan), 5 mM (blue), 10 mM (red), 20 mM (light green), 50 mM (black), and 100 mM (dark green) D-histidine. All traces were fit with eq 1. Time indicated is after the end of the flow, i.e., 2 ms. For clarity one experimental point every 10 is shown (vertical lines). Panel B shows the observed rate of flavin reduction as a function of D-histidine concentration. Data were fit to eq 2.

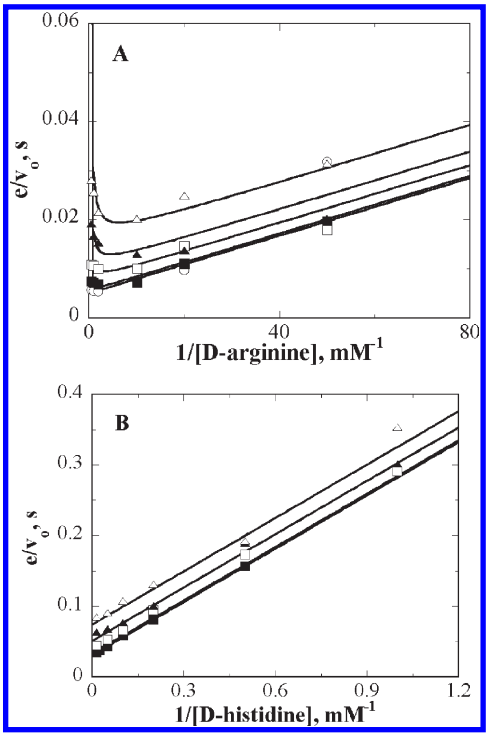

FIGURE 3: Steady-state kinetics for the oxidation D-arginine (panel A) or D-histidine (panel B) catalyzed by D-arginine dehydrogenase. Initial rates of reaction were measured at varying concentrations of both the amino acid substrate and PMS in 20 mM Tris-HCl, pH 8.7, at 25 °C. Panel A: Concentrations of PMS were (○) 500 μM, (■) 100 μM, (□) 20 μM, (▲) 10 μM, and (Δ) 5 μM. Data were fit to eq 3. Panel B: Concentrations of PMS were (■) 100 μM, (□) 50 μM, (▲) 10 μM, and (Δ) 5 μM. Data were fit to eq 4.

constant for flavin reduction ($k_{red} = 60 \pm 1\ s^{-1}$) and the apparent equilibrium constant for substrate dissociation at the active site of the enzyme ($^{app}K_d = 10 \pm 1$ mM). The best fit of the data was obtained with the curve extrapolating to a *y*-intercept value of zero, consistent with an irreversible reduction of the flavin.

Steady-State Kinetic Mechanism. The steady-state kinetic mechanism and the associated kinetic parameters of the enzyme were determined using the method of the initial rates (*14*). The rate of oxygen consumption was measured at varying concentrations of either D-arginine or D-histidine and the artificial electron acceptor PMS, in 20 mM Tris-HCl at pH 8.7 and 25 °C. As illustrated in Figure 3, parallel lines were obtained in double reciprocal plots of the enzymatic rate versus the concentration of the amino acid substrate, with significant substrate inhibition at concentrations of D-arginine ≥0.5 mM. Substrate inhibition was also seen with PMS at concentrations of D-arginine equal to, or lower than, 50 μM (data not shown). Nonetheless, the best fit of the data with D-arginine was obtained by using eq 3, which describes a ping-pong bi-bi steady-state kinetic mechanism with inhibition by D-arginine (*13*). The best fit of the data with D-histidine was obtained by using eq 4, consistent with a ping-pong bi-bi steady-state kinetic mechanism and no substrate inhibition. As summarized in Table 2, the overall rate of enzymatic turnover determined with D-arginine at saturating concentrations of both substrates (k_{cat}) was ~200 s^{-1}, a value that was 6-fold larger than the k_{cat} value of 35 s^{-1} determined when D-histidine was used as substrate. The second-order rate constant for the capture of D-arginine to yield enzyme−substrate complexes committed to catalysis (i.e., k_{cat}/K_{Arg}) was in the 10^6 M^{-1} s^{-1} range, which was 850-fold larger than the corresponding value of 4000 M^{-1} s^{-1} determined with D-histidine. These data establish that D-histidine is significantly slower than D-arginine as a substrate.

Table 2: Kinetic Parameters of D-Arginine Dehydrogenase with D-Arginine and D-Histidine[a]

kinetic parameter[b]	D-arginine	D-histidine
k_{cat}, s^{-1}	204 ± 3	35 ± 3
K_a, mM	0.06 ± 0.01	8.8 ± 0.5
K_b, μM	11 ± 2	8.0 ± 0.6
k_{cat}/K_a, M^{-1} s^{-1}	(3.4 ± 0.3) × 10^6	4,000 ± 300
k_{cat}/K_b, M^{-1} s^{-1}	(1.9 ± 0.3) × 10^7	(4.4 ± 0.3) × 10^6
$K_{i\text{-}A}$, mM	0.9 ± 0.3	no[c]
k_{red}, s^{-1}	≥700[d]	60 ± 1
K_d, mM	≤0.05[e]	10 ± 1

[a]Enzyme activity was measured at varying concentrations of both D-arginine or D-histidine and PMS in 20 mM Tris-HCl, pH 8.7, at 25 °C. [b]Kinetic data are readily accounted for with the kinetic mechanism of Scheme 2. [c]Not observed. [d]Estimated lower limiting value. [e]Estimated upper limiting value. The reaction occurs within the dead time of the spectrometer and thus cannot be accurately measured by stopped-flow techniques.

Solvent Viscosity Effect. The effects of solvent viscosity on the k_{cat} and k_{cat}/K_m values with D-arginine and D-histidine were investigated to determine whether diffusion-controlled events influenced the binding of the substrate and the release of the product to and from the enzyme. With D-arginine as substrate, when the reciprocals of the normalized k_{cat}/K_m values determined at increasing concentrations of glycerol were plotted as a function

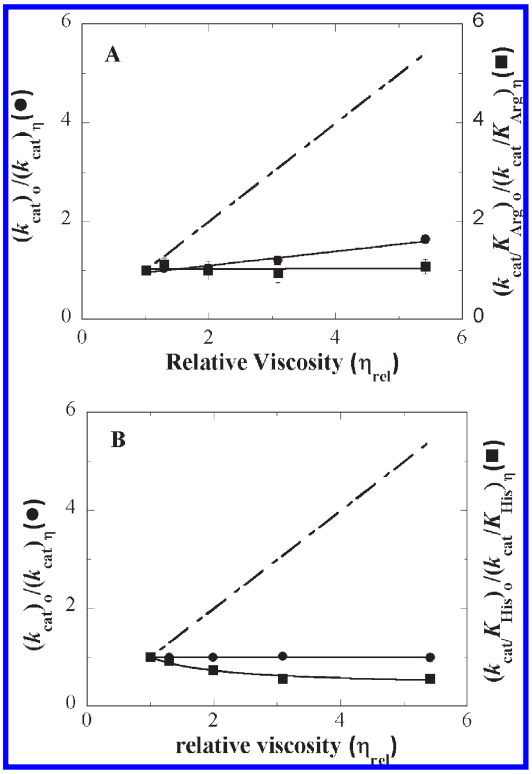

FIGURE 4: Effects of solvent viscosity on the steady-state kinetic parameters for the D-arginine dehydrogenase with D-arginine or D-histidine as a substrate. Panel A shows the normalized k_{cat} (●) and k_{cat}/K_m (■) values with D-arginine as a function of the relative solvent viscosity. Panel B shows the normalized k_{cat} (●) and k_{cat}/K_m (■) values with D-histidine as a function of the relative solvent viscosity. The dashed lines with a slope of 1 indicate the expected results for a fully diffusion-limited reaction. The values for the relative viscosities of the solvent were taken from Weast (*12*) and adjusted for 25 °C. Reaction rates were measured at varying concentrations of D-arginine or D-histidine and fixed 1 mM PMS in 20 mM Tris-HCl, pH 8.7, at 25 °C.

of the relative viscosity, the data yielded a line with negligible slope (i.e., 0.004 ± 0.022) (Figure 4A). In contrast, a line with slope of 0.14 ± 0.02 was obtained in a plot of the normalized k_{cat} value (Figure 4A). With D-histidine, the normalized k_{cat} values were independent of solvent viscosity; in contrast, the k_{cat}/K_m values increased with increasing viscosity yielding an inverse hyperbolic pattern in a plot of the $(k_{cat}/K_m)_0/(k_{cat}/K_m)_\eta$ values versus relative viscosity (Figure 4B). These data establish that kinetic steps involving substrate binding and product release are affected in different fashions by solvent viscosity when the enzyme turns over with D-arginine or D-histidine.

DISCUSSION

Steady-State Kinetic Mechanism. The steady-state kinetic mechanism of D-arginine dehydrogenase has been determined with D-arginine and D-histidine as substrates at pH 8.7 and is consistent with the minimal ping-pong bi-bi mechanism illustrated in Scheme 2. After the formation of the Michaelis complex $DADH_{ox}\cdot S$, the amino acid substrate is oxidized to the corresponding imino acid with concomitant reduction of the enzyme-bound flavin ($DADH_{red}\cdot P$). Release of the imino product from the active site of the enzyme completes the reductive half-reaction. The oxidative half-reaction with the artificial electron acceptor PMS occurs through the initial formation of a Michaelis complex $DADH_{red}\cdot PMS$, within which catalysis yields the $DADH_{ox}\cdot PMSH_2$ complex. Turnover is then completed

Scheme 2: Proposed Steady-State Kinetic Mechanism for the Oxidation of D-Arginine Catalyzed by D-Arginine Dehydrogenase[a]

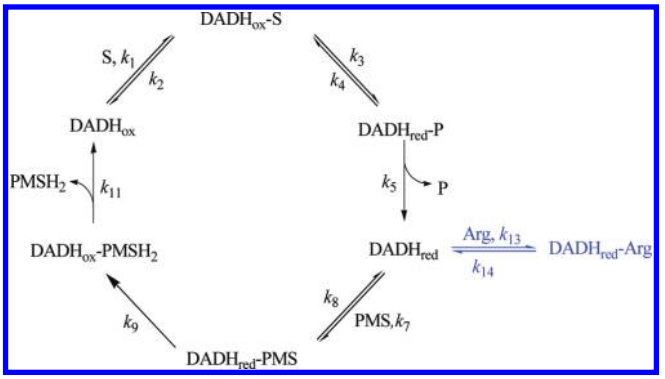

[a]$DADH_{ox}$, oxidized D-arginine dehydrogenase; S, substrate; $DADH_{red}$, reduced D-arginine dehydrogenase; P, imino product; $PMSH_2$, reduced phenazine methosulfate; Arg, D-arginine; k_5 and k_{11} are shown as irreversible because initial rates are measured in the absence of products; k_4, although shown, is close to zero as suggested by stopped-flow kinetic data (see text); k_9 is shown as irreversible based on the oxidation−reduction potential of $PMS/PMSH_2 > FAD/FADH_2$, with values of +80 and −200 mV (*60*), respectively.

with the release of reduced PMS from the oxidized enzyme. Evidence in support of a ping-pong kinetic mechanism comes from the steady-state kinetic data determined at varying concentrations of D-arginine or D-histidine and PMS and from the substrate inhibition of enzymatic turnover at high concentrations of D-arginine. First, the parallel lines observed in the plots of the reciprocal of the initial rates of reaction as a function of the reciprocal of the substrate concentrations are consistent with the irreversible step of product release (k_5) occurring before binding of PMS to the reduced enzyme (k_7). D-Arginine inhibition of turnover is readily explained with the formation of a dead-end complex $DADH_{red}\cdot Arg$ when D-arginine at high concentrations binds to the free reduced enzyme (in blue in Scheme 2). In agreement with a ping-pong kinetic mechanism where PMS reacts with the reduced enzyme after the iminoarginine product of the reaction is released from the enzyme active site, the K_{PMS} had similar values irrespective of whether D-histidine or D-arginine was the substrate, namely, ~10 μM (Table 2).

In principle, a kinetic pattern with parallel lines could also be obtained with PMS binding to a $DADH_{red}\cdot P$ complex formed by an irreversible conversion of the $DADH_{ox}\cdot S$ complex (*15*). If this were the case, D-arginine inhibition of turnover would require the formation of either a ternary complex of the enzyme with two D-arginines or a quaternary complex of the enzyme, PMS and two D-arginines. Both these possibilities appear very unlikely since the available crystallographic structure of the enzyme cocrystallized with D-arginine shows that the active site cavity of the enzyme is almost entirely occupied with a single iminoarginine, thereby preventing the binding of a second arginine (*9*). Inhibition of catalytic turnover due to formation of a dead-end complex between the substrate and the reduced form of the enzyme was previously observed in other flavoproteins, such as nitroalkane oxidase (*16*), aldehyde oxidase (*17*), flavocytochrome b_2 (*18*), cellobiose dehydrogenase (*19*), and thymidylate synthase (*20*).

Substrate Binding. Binding of the D-amino acid substrate to the oxidized enzyme occurs in rapid equilibrium. This establishes that the rate constant for the dissociation of the D-amino acid from the $DADH_{ox}\cdot S$ complex destined for catalysis (k_2) must be

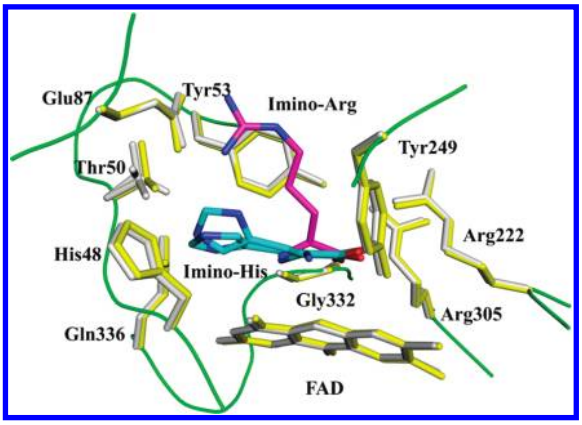

FIGURE 5: Structural comparison of active sites of D-arginine dehydrogenase/iminoarginine (yellow) and D-arginine dehydrogenase/iminohistidine (gray). Active site residues and FAD molecule are represented as sticks. The protein main chain is shown as a green coil.

significantly larger than the rate constant for its oxidation to yield the products of the reaction (k_3). Evidence to support this conclusion comes from the solvent viscosity effects on the second-order rate constants for the capture of D-arginine or D-histidine onto the enzyme to yield complexes committed to catalysis (k_{cat}/K_{Arg} and k_{cat}/K_{His}) (Figure 4). These data are readily explained if one considers that a line with a slope between zero and +1 would be expected in a plot of the normalized k_{cat}/K_m values as a function of increasing relative viscosity of the solvent for a reductive half-reaction whose overall rate was at least partially controlled by the diffusion of the substrate in the active site of the enzyme (*21*). Such a linear dependence of the normalized k_{cat}/K_m values on solvent viscosity was not observed with D-arginine dehydrogenase, for which the solvent viscosity effect was either negligible with a slope not significantly different from zero in the case of D-arginine or inverse and hyperbolic in the case of D-histidine (Figure 4). The lack of a solvent viscosity effect on the k_{cat}/K_{Arg} value is somewhat surprising because large k_{cat}/K_m values in the range of 10^6 M^{-1} s^{-1} like the one determined here with D-arginine are commonly associated with some degree of diffusion control for the binding of substrates to enzymes (*22*−*25*).

Substrate binding to the oxidized enzyme in rapid equilibrium immediately establishes the $^{app}K_d$ values determined in the stopped-flow spectrophotometer as the true dissociation constants reporting on the thermodynamic equilibrium of the free oxidized enzyme and the Michaelis enzyme−substrate complex (i.e., $K_d = k_2/k_1$) (Scheme 2). Although an accurate determination of the K_d value with D-arginine could not be obtained due to the reaction being too fast to be followed with a stopped-flow spectrophotometer, the rapid kinetic data on the reductive half-reaction suggest a K_d value for D-arginine lower than 50 μM. Thus, binding of D-arginine in the active site of the enzyme is at least 200-fold tighter than that of D-histidine, with a K_d value of 10 mM. Tighter binding of D-arginine to D-arginine dehydrogenase as compared to D-histidine is primarily due to the favorable electrostatic interaction of the guanidinium side chain of D-arginine with the active site residue Glu87; such an interaction is not present with D-histidine, as suggested by the structures of the enzyme in complex with iminoarginine and iminohistidine recently reported (Figure 5) (*9*). The importance of an electrostatic interaction involving a glutamate residue for selective binding of the substrate in the active site of a flavoenzyme was recently established in choline oxidase through mechanistic and structural studies (*11*). In that case, site-directed mutagenesis studies or the use of substrate analogues devoid of charge was

Scheme 3: Isomerization of the Michaelis Complex with D-Histidine[a]

$$DADH_{ox} \underset{k_2}{\overset{His,\ k_1}{\rightleftharpoons}} DADH_{ox}\text{-}His \underset{K_{iso}}{\rightleftharpoons} DADH_{ox}\text{-}His^{*} \underset{k_4}{\overset{k_3}{\rightleftharpoons}} DADH_{red}\text{-}P \xrightarrow[P]{k_5} DADH_{red}$$

[a] $DADH_{ox}$, oxidized D-arginine dehydrogenase; His, D-histidine; $DADH_{red}$, reduced D-arginine dehydrogenase; P, iminohistidine.

consistent with a ~15 kJ mol^{-1} energetic contribution of the side chain of Glu312 to the ionic interaction with the positively charged choline (*11*). A comparable energetic contribution to substrate binding is likely provided by Glu87 in D-arginine dehydrogenase, as suggested by the at least 200-fold ratio of the K_d values estimated for D-arginine and D-histidine.

Isomerization of the Michaelis Complex with D-Histidine. After the initial formation of the Michaelis complex involving the oxidized enzyme and D-histidine, the $DADH_{ox}$·His species isomerizes to produce an enzyme−substrate complex $DADH_{ox}$·His* that is competent for the subsequent reaction of flavin reduction (Scheme 3). Evidence for this conclusion comes from the effect of increasing solvent viscosity on the normalized k_{cat}/K_{His} values determined in the presence of glycerol. The k_{cat}/K_{His} values increased hyperbolically to a limiting value with increasing viscosity of the solvent (Figure 4), consistent with the presence of an internal equilibrium of the enzyme−substrate complex in the reductive half-reaction. Moreover, in the crystal structure of D-arginine dehydrogenase in complex with iminohistidine, the ligand is present in two conformations with respect to the flavin (Figure 5) (*9*). One of the two conformations presents the imino group of iminohistidine in the same orientation relative to the flavin 7,8-dimethylisoalloxazine that is seen in the crystal structure of the enzyme in complex with iminoarginine (Figure 5) (*9*). This conformation is likely to be competent for catalysis in the enzyme−substrate complex. The alternative conformation most likely is not competent for the subsequent reaction of flavin reduction, as suggested by the relative orientation of groups participating in the hydride transfer reaction. Thus, the isomerization of the $DADH_{ox}$·His complex can be readily explained as reflecting the reversible conversion of multiple binding conformations, not all of which are catalytically competent for the subsequent oxidation reaction involving the flavin. The isomerization of the $DADH_{ox}$·S complex is not observed with D-arginine as substrate. This stems from a more optimal binding mode of D-arginine as compared to D-histidine, which also exploits the extra interaction of the positively charged side chain with the active site Glu87 (*vide ante*) (Figure 5) (*9*). Isomerizations of Michaelis complexes prior to the reaction of flavin reduction have been previously observed in the wild type and selected mutant forms of flavocytochrome b_2 (*26*) and in a mutant form of choline oxidase where the active site Glu312 is replaced with aspartate (*11*).

Flavin Reduction. The oxidation of the amino acid substrate catalyzed by D-arginine dehydrogenase entails the two-electron, irreversible reduction of the enzyme-bound flavin without formation of any observable reaction intermediates. Evidence for this conclusion comes from the rapid kinetic data on the reductive half-reaction determined in a stopped-flow spectrophotometer, yielding a monophasic decrease in the absorbance of FAD when the enzyme is mixed with D-histidine as substrate. Irreversibility of the flavin reduction (i.e., k_4 being close to zero in Scheme 2) is established from the extrapolation to the origin of the hyperbolic

dependence of the k_{obs} values as a function of the concentration of the D-histidine substrate (*27*). Lack of observable reaction intermediates implies that if they were formed, they would have to decay at rates that are at least 20 times faster than their rates of formation. Although alternate mechanisms for flavin reduction cannot be ruled out at this stage, these observations are consistent with the mechanism for substrate oxidation by hydride transfer that has been previously proposed for other flavoproteins acting on amino acids, such as D-amino acid oxidase (*28*, *29*) and sarcosine oxidase (*29*), α-hydroxy acids, such as flavocytochrome b_2 (*26*, *30*, *31*), or alcohol substrates, such as choline oxidase (*32*, *33*), aryl alcohol oxidase (*34*), and pyranose 2-oxidase (*35*).

The oxidation of D-arginine by D-arginine dehydrogenase is at least 20 times faster than the oxidation of D-histidine, as indicated by the rate constants for flavin reduction estimated upon mixing the enzyme and the substrate in the stopped-flow spectrophotometer. The larger k_{red} value seen with D-arginine likely originates from a better orientation and positioning in the active site of D-arginine with respect to D-histidine, due to the favorable interaction of its side chain with Glu87 (Figure 5) (*9*). The importance of substrate orientation and positioning for efficient oxidation of an organic molecule has been recently established in another flavoprotein, choline oxidase, where it was shown that the conservative replacement of an active site Glu with Asp results in a 230-fold decrease in the k_{red} value for the oxidation of the alcohol substrate (*11*).

Product Release. With D-arginine as substrate, the release of iminoarginine from the active site of the enzyme is partially rate limiting for the overall turnover of the enzyme. This conclusion is supported by the effect of increasing solvent viscosity on the normalized rate constant for the overall turnover number of the enzyme at saturating concentrations of D-arginine and PMS (i.e., k_{cat}). The reaction would be slower in solvents with higher viscosities if a diffusion-controlled process is the rate-limiting step (*36*). Since product release is the only diffusive step during turnover when the enzyme is saturated with substrates, a line with a slope of 0.14 as observed in Figure 4 indicates that the release of the product is partially rate limiting in turnover. In contrast, enzymatic turnover with D-histidine is not limited by the rate of product release from the enzyme active site, as suggested by the lack of solvent viscosity effects on the k_{cat} value with D-histidine. Instead, the overall turnover of the enzyme with D-histidine is at least partially limited by the kinetic step of flavin reduction, as suggested by the comparison of the k_{red} value of 60 s^{-1} determined by using rapid reaction kinetics and the k_{cat} value of 35 s^{-1} determined by using the steady-state kinetic approach.

Lack of Oxygen Reactivity. D-Arginine dehydrogenase is a true dehydrogenase that reacts very poorly, if at all, with molecular oxygen. This conclusion is supported by the lack of oxygen consumption observed upon mixing the enzyme with D-arginine or with 15 other D-amino acids at pH 8.7 as determined by using a Clark-type oxygen electrode. In contrast, an initial rate of ~800 s^{-1} was observed upon addition of 1 mM PMS as an electron acceptor to the same reaction mixture, identifying the enzyme as a true dehydrogenase.

The analysis of the crystal structure of the enzyme and its comparison with that of D-amino acid oxidase, which readily reacts with oxygen (i.e., $k_{cat}/K_{oxygen} = 10^5$ M^{-1} s^{-1}) (*37*), helps to rationalize the lack of oxygen reactivity in D-arginine dehydrogenase. First, the methyl side chain of Ala46 appears to physically block access of oxygen to the reactive C(4a) atom of the flavin in the active site of D-arginine dehydrogenase (Figure 6). The

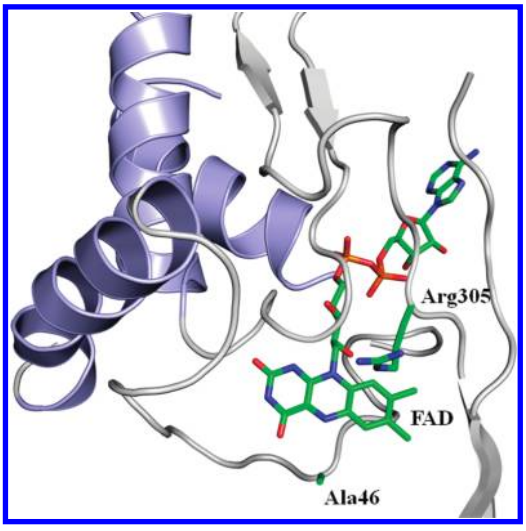

FIGURE 6: Active site of D-arginine dehydrogenase (PDB number 3NYE) (*9*). For clarity, only selected amino acid residues are shown. The FAD cofactor is shown as a stick representation. The side chain of Ala46 is shown in green.

corresponding residue in D-amino acid oxidase is Gly52 (with the numbering of the enzyme from *Rhodotorula gracilis*) (*38*). When Gly52 is replaced with a bulkier Val, the resulting mutant enzyme loses the ability to react with oxygen due to steric hindrance preventing oxygen access to the reduced flavin (*38*). The importance of permitting physical access of oxygen to the C(4a) atom of the flavin has also been shown with site-directed mutagenesis in L-galactono-γ-lactone dehydrogenase (*39*, *40*). In the wild-type enzyme, which reacts poorly with oxygen, access to the C(4a) atom of the flavin is blocked by the side chain of Ala113. However, replacement of this residue with a smaller Gly yields a 400-fold increase of the k_{cat}/K_{oxygen} to 3.4×10^5 M^{-1} s^{-1}, a value that is typically found in oxidases (*39*).

Lack of oxygen reactivity in D-arginine dehydrogenase is also most likely associated with the absence of positive charges in close proximity of the C(4a) and N(1)−C(2) atoms of the flavin. In this regard, the positive charge of the substrate/product of D-arginine dehydrogenase can be immediately ruled out since the ping-pong steady-state kinetic mechanism establishes that the reaction of the reduced flavin with the electron acceptor occurs on the enzyme after the release of the reaction product from the enzyme. The positive charge of Arg305 is the closest to both the C(4a) and N(1)−C(2) atoms of the flavin, at distances ≥7 Å (Figure 6). In some oxidases the N-terminal end of an α-helix providing a partial positive charge either reinforces or substitutes for the effect of the full positive charge proximal to the flavin N(1)−C(2) atoms, as exemplified by D-amino acid oxidase (*41*−*43*), cholesterol oxidase (*44*), and polyamine oxidase (*45*). However, in D-arginine dehydrogenase the closest α-helix is 6 Å away from the N(1)−C(2) atoms of the flavin and points in the opposite direction (Figure 6). These positive charges, which are typical in several flavoprotein oxidases (*46*−*52*), exert two independent roles. The positive charge close to the flavin C(4a) atom has been proposed to facilitate the stabilization of the negatively charged superoxide species that transiently forms in the reaction of the reduced flavin with oxygen. This has been established in a number of flavoprotein oxidases by using mechanistic and structural approaches, among which are glucose oxidase (*53*), monoamine oxidase (*54*, *55*), monomeric sarcosine oxidase (*56*), and choline oxidase (*57*, *58*). The positive charge close to the N(1)−C(2) atoms

of the flavin has been proposed to provide electrostatic stabilization of the anionic hydroquinone form of the reduced flavin, which is a common feature in flavoprotein oxidases but not in dehydrogenases (*59*).

Conclusions. In summary, we have engineered an untagged form of D-arginine dehydrogenase, purified it to high levels, and investigated its steady-state kinetic mechanism and reductive half-reaction with the substrates D-arginine and D-histidine. The results of the kinetic investigation show that the enzyme is a true dehydrogenase that does not react in its reduced state with molecular oxygen. With both amino acid substrates the enzyme displays a ping-pong bi-bi kinetic mechanism when PMS is used as electron acceptor. Flavin reduction is partially rate limiting for the overall turnover of the enzyme with the slow substrate D-histidine but not with the fast substrate D-arginine. With the latter, release of the iminoarginine product of the oxidation of D-arginine from the active site of the enzyme is partially rate limiting for the overall turnover of the enzyme. An isomerization of the Michaelis complex is also established with D-histidine prior to the flavin kinetic step, likely reflecting the conversion of multiple binding conformations that are not all catalytically competent for the subsequent flavin reduction. The kinetic investigation of the authentic untagged form of D-arginine dehydrogenase reported herein, along with the recent structural investigation of the iminoarginine− and iminohistidine−enzyme complexes at high resolutions, will provide a solid framework for future mutagenesis and mechanistic studies aimed at the characterization of the enzyme.

ACKNOWLEDGMENT

The authors thank Prof. Chung-Dar Lu and Dr. Congran Li for the kind gift of plasmid pCR3 harboring the *dauA* gene encoding for D-arginine dehydrogenase. We thank Dr. Andrea Pennati and Mr. Kevin Francis for critical reading of the manuscript.

REFERENCES

1. Li, C., and Lu, C. D. (2009) Arginine racemization by coupled catabolic and anabolic dehydrogenases. *Proc. Natl. Acad. Sci. U.S.A. 106*, 906–911.
2. Jann, A., Matsumoto, H., and Haas, D. (1988) The fourth arginine catabolic pathway of *Pseudomonas aeruginosa*. *J. Gen. Microbiol. 134*, 1043–1053.
3. Olsiewski, P. J., Kaczorowski, G. J., and Walsh, C. (1980) Purification and properties of D-amino acid dehydrogenase, an inducible membrane-bound iron-sulfur flavoenzyme from *Escherichia coli* B. *J. Biol. Chem. 255*, 4487–4494.
4. White, T. A., Krishnan, N., Becker, D. F., and Tanner, J. J. (2007) Structure and kinetics of monofunctional proline dehydrogenase from *Thermus thermophilus*. *J. Biol. Chem. 282*, 14316–14327.
5. Li, C., Yao, X., and Lu, C. D (2010) Regulation of the dauBAR operon and characterization of D-amino acid dehydrogenase DauA in arginine and lysine catabolism of *Pseudomonas aeruginosa* PAO1. *Microbiology 156*, 60–71.
6. Boselli, A., Piubelli, L., Molla, G., Sacchi, S., Pilone, M. S., Ghisla, S., and Pollegioni, L. (2004) On the mechanism of *Rhodotorula gracilis* D-amino acid oxidase: role of the active site serine 335. *Biochim. Biophys. Acta 1702*, 19–32.
7. Krebs, H. A. (1935) Metabolism of amino-acids: deamination of amino-acids. *Biochem. J. 29*, 1620–1644.
8. Vanoni, M. A., Cosma, A., Mazzeo, D., Mattevi, A., Todone, F., and Curti, B. (1997) Limited proteolysis and X-ray crystallography reveal the origin of substrate specificity and of the rate-limiting product release during oxidation of D-amino acids catalyzed by mammalian D-amino acid oxidase. *Biochemistry 36*, 5624–5632.
9. Fu, G., Yuan, H., Li, C., Lu, C. D., Gadda, G., Weber, I. T (2010) Conformational changes and substrate recognition in *Pseudomonas aeruginosa* D-arginine dehydrogenase, *Biochemistry* (in press).
10. Bradford, M. M. (1976) A rapid and sensitive method for the quantitation of microgram quantities of protein utilizing the principle of protein-dye binding. *Anal. Biochem. 72*, 248–254.
11. Quaye, O., Lountos, G. T., Fan, F., Orville, A. M., and Gadda, G. (2008) Role of Glu312 in binding and positioning of the substrate for the hydride transfer reaction in choline oxidase. *Biochemistry 47*, 243–256.
12. Weast, R. C. (1981) Handbook of Chemistry and Physics, Chemical Rubber Publishing Co. (CRC Press), Boca Raton, FL.
13. Cook, P. F., and Cleland, W. W. (2007) Enzyme Kinetics and Mechanism, Garland Science Publishing, New York, NY.
14. Gadda, G., and McAllister-Wilkins, E. E. (2003) Cloning, expression, and purification of choline dehydrogenase from the moderate halophile *Halomonas elongata*. *Appl. Environ. Microbiol. 69*, 2126–2132.
15. Rungsrisuriyachai, K., and Gadda, G. (2009) A pH switch affects the steady-state kinetic mechanism of pyranose 2-oxidase from *Trametes ochracea*. *Arch. Biochem. Biophys. 483*, 10–15.
16. Gadda, G., and Fitzpatrick, P. F. (2000) Iso-mechanism of nitroalkane oxidase: 1. Inhibition studies and activation by imidazole. *Biochemistry 39*, 1400–1405.
17. Itoh, K., Asakawa, T., Hoshino, K., Adachi, M., Fukiya, K., Watanabe, N., and Tanaka, Y. (2009) Functional analysis of aldehyde oxidase using expressed chimeric enzyme between monkey and rat. *Biol. Pharm. Bull. 32*, 31–35.
18. Rouviere, N., Mayer, M., Tegoni, M., Capeillere-Blandin, C., and Lederer, F. (1997) Molecular interpretation of inhibition by excess substrate in flavocytochrome b_2: a study with wild-type and Y143F mutant enzymes. *Biochemistry 36*, 7126–7135.
19. Igarashi, K., Momohara, I., Nishino, T., and Samejima, M. (2002) Kinetics of inter-domain electron transfer in flavocytochrome cellobiose dehydrogenase from the white-rot fungus Phanerochaete chrysosporium. *Biochem. J. 365*, 521–526.
20. Wang, Z., Chernyshev, A., Koehn, E. M., Manuel, T. D., Lesley, S. A., and Kohen, A. (2009) Oxidase activity of a flavin-dependent thymidylate synthase. *FEBS J. 276*, 2801–2810.
21. Gavish, B., and Werber, M. M. (1979) Viscosity-dependent structural fluctuations in enzyme catalysis. *Biochemistry 18*, 1269–1275.
22. Mattei, P., Kast, P., and Hilvert, D. (1999) *Bacillus subtilis* chorismate mutase is partially diffusion-controlled. *Eur. J. Biochem. 261*, 25–32.
23. Shih, M. J., Edinger, J. W., and Creighton, D. J. (1997) Diffusion-dependent kinetic properties of glyoxalase I and estimates of the steady-state concentrations of glyoxalase-pathway intermediates in glycolyzing erythrocytes. *Eur. J. Biochem. 244*, 852–857.
24. Lin, Y., Volkman, J., Nicholas, K. M., Yamamoto, T., Eguchi, T., Nimmo, S. L., West, A. H., and Cook, P. F. (2008) Chemical mechanism of homoisocitrate dehydrogenase from *Saccharomyces cerevisiae*. *Biochemistry 47*, 4169–4180.
25. Wood, B. M., Chan, K. K., Amyes, T. L., Richard, J. P., and Gerlt, J. A. (2009) Mechanism of the orotidine 5′-monophosphate decarboxylase-catalyzed reaction: effect of solvent viscosity on kinetic constants. *Biochemistry 48*, 5510–5517.
26. Sobrado, P., and Fitzpatrick, P. F. (2003) Solvent and primary deuterium isotope effects show that lactate CH and OH bond cleavages are concerted in Y254F flavocytochrome b_2, consistent with a hydride transfer mechanism. *Biochemistry 42*, 15208–15214.
27. Strickland, S., Palmer, G., and Massey, V. (1975) Determination of dissociation constants and specific rate constants of enzyme-substrate (or protein-ligand) interactions from rapid reaction kinetic data. *J. Biol. Chem. 250*, 4048–4052.
28. Fitzpatrick, P. F. (2004) Carbanion versus hydride transfer mechanisms in flavoprotein-catalyzed dehydrogenations. *Bioorg. Chem. 32*, 125–139.
29. Fitzpatrick, P. F. (2010) Oxidation of amines by flavoproteins. *Arch. Biochem. Biophys. 493*, 13–25.
30. Mowat, C. G., Wehenkel, A., Green, A. J., Walkinshaw, M. D., Reid, G. A., and Chapman, S. K. (2004) Altered substrate specificity in flavocytochrome b_2: structural insights into the mechanism of L-lactate dehydrogenation. *Biochemistry 43*, 9519–9526.
31. Tabacchi, G., Zucchini, D., Caprini, G., Gamba, A., Lederer, F., Vanoni, M. A., and Fois, E. (2009) L-lactate dehydrogenation in flavocytochrome b_2: a first principles molecular dynamics study. *FEBS J. 276*, 2368–2380.
32. Fan, F., and Gadda, G. (2005) On the catalytic mechanism of choline oxidase. *J. Am. Chem. Soc. 127*, 2067–2074.
33. Gadda, G. (2008) Hydride transfer made easy in the reaction of alcohol oxidation catalyzed by flavin-dependent oxidases. *Biochemistry 47*, 13745–13753.
34. Ferreira, P., Hernandez-Ortega, A., Herguedas, B., Rencoret, J., Gutierrez, A., Martinez, M. J., Jimenez-Barbero, J., Medina, M.,

and Martinez, A. T. (2010) Kinetic and chemical characterization of aldehyde oxidation by fungal aryl-alcohol oxidase. *Biochem. J. 425*, 585–593.
35. Sucharitakul, J., Wongnate, T., and Chaiyen, P. (2010) Kinetic isotope effects on the noncovalent flavin mutant protein of pyranose 2-oxidase reveal insights into the flavin reduction mechanism. *Biochemistry 49*, 3753–3765.
36. Blacklow, S. C., Raines, R. T., Lim, W. A., Zamore, P. D., and Knowles, J. R. (1988) Triosephosphate isomerase catalysis is diffusion controlled. Appendix: Analysis of triose phosphate equilibria in aqueous solution by ^{31}P NMR. *Biochemistry 27*, 1158–1167.
37. Pollegioni, L., Langkau, B., Tischer, W., Ghisla, S., and Pilone, M. S. (1993) Kinetic mechanism of D-amino acid oxidases from *Rhodotorula gracilis* and *Trigonopsis variabilis*. *J. Biol. Chem. 268*, 13850–13857.
38. Saam, J., Rosini, E., Molla, G., Schulten, K., Pollegioni, L., and Ghisla, S. (2010) O_2-reactivity of flavoproteins: dynamic access of dioxygen to the active site and role of a H^+ relay system in D-amino acid oxidase. *J. Biol. Chem. 285*, 24439–24446.
39. Leferink, N. G., Fraaije, M. W., Joosten, H. J., Schaap, P. J., Mattevi, A., and van Berkel, W. J. (2009) Identification of a gatekeeper residue that prevents dehydrogenases from acting as oxidases. *J. Biol. Chem. 284*, 4392–4397.
40. Baron, R., Riley, C., Chenprakhon, P., Thotsaporn, K., Winter, R. T., Alfieri, A., Forneris, F., van Berkel, W. J., Chaiyen, P., Fraaije, M. W., Mattevi, A., and McCammon, J. A. (2009) Multiple pathways guide oxygen diffusion into flavoenzyme active sites. *Proc. Natl. Acad. Sci. U.S.A. 106*, 10603–10608.
41. Mattevi, A., Vanoni, M. A., Todone, F., Rizzi, M., Teplyakov, A., Coda, A., Bolognesi, M., and Curti, B. (1996) Crystal structure of D-amino acid oxidase: a case of active site mirror-image convergent evolution with flavocytochrome b_2. *Proc. Natl. Acad. Sci. U.S.A. 93*, 7496–7501.
42. Fitzpatrick, P. F., and Massey, V. (1983) The reaction of 8-mercaptoflavins and flavoproteins with sulfite. Evidence for the role of an active site arginine in D-amino acid oxidase. *J. Biol. Chem. 258*, 9700–9705.
43. Porter, D. J., Voet, J. G., and Bright, H. J. (1977) Mechanistic features of the D-amino acid oxidase reaction studied by double stopped flow spectrophotometry. *J. Biol. Chem. 252*, 4464–4473.
44. Li, J., Vrielink, A., Brick, P., and Blow, D. M. (1993) Crystal structure of cholesterol oxidase complexed with a steroid substrate: implications for flavin adenine dinucleotide dependent alcohol oxidases. *Biochemistry 32*, 11507–11515.
45. Binda, C., Coda, A., Angelini, R., Federico, R., Ascenzi, P., and Mattevi, A. (1999) A 30-angstrom-long U-shaped catalytic tunnel in the crystal structure of polyamine oxidase. *Structure 7*, 265–276.
46. Xia, Z. X., and Mathews, F. S. (1990) Molecular structure of flavocytochrome b_2 at 2.4 Å resolution. *J. Mol. Biol. 212*, 837–863.
47. Barber, M. J., Neame, P. J., Lim, L. W., White, S., and Matthews, F. S. (1992) Correlation of x-ray deduced and experimental amino acid sequences of trimethylamine dehydrogenase. *J. Biol. Chem. 267*, 6611–6619.
48. Mattevi, A., Fraaije, M. W., Mozzarelli, A., Olivi, L., Coda, A., and van Berkel, W. J. (1997) Crystal structures and inhibitor binding in the octameric flavoenzyme vanillyl-alcohol oxidase: the shape of the active-site cavity controls substrate specificity. *Structure 5*, 907–920.
49. Stenberg, K., and Lindqvist, Y. (1997) Three-dimensional structures of glycolate oxidase with bound active-site inhibitors. *Protein Sci. 6*, 1009–1015.
50. Fox, K. M., and Karplus, P. A. (1994) Old yellow enzyme at 2 Å resolution: overall structure, ligand binding, and comparison with related flavoproteins. *Structure 2*, 1089–1105.
51. Rowland, P., Bjornberg, O., Nielsen, F. S., Jensen, K. F., and Larsen, S. (1998) The crystal structure of *Lactococcus lactis* dihydroorotate dehydrogenase A complexed with the enzyme reaction product throws light on its enzymatic function. *Protein Sci. 7*, 1269–1279.
52. Benson, T. E., Walsh, C. T., and Hogle, J. M. (1997) X-ray crystal structures of the S229A mutant and wild-type MurB in the presence of the substrate enolpyruvyl-UDP-*N*-acetylglucosamine at 1.8-Å resolution. *Biochemistry 36*, 806–811.
53. Roth, J. P., and Klinman, J. P. (2003) Catalysis of electron transfer during activation of O2 by the flavoprotein glucose oxidase. *Proc. Natl. Acad. Sci. U.S.A. 100*, 62–67.
54. Tan, A. K., and Ramsay, R. R. (1993) Substrate-specific enhancement of the oxidative half-reaction of monoamine oxidase. *Biochemistry 32*, 2137–2143.
55. Miller, J. R., and Edmondson, D. E. (1999) Influence of flavin analogue structure on the catalytic activities and flavinylation reactions of recombinant human liver monoamine oxidases A and B. *J. Biol. Chem. 274*, 23515–23525.
56. Zhao, G., Bruckner, R. C., and Jorns, M. S. (2008) Identification of the oxygen activation site in monomeric sarcosine oxidase: role of Lys265 in catalysis. *Biochemistry 47*, 9124–9135.
57. Gadda, G., Powell, N. L., and Menon, P. (2004) The trimethylammonium headgroup of choline is a major determinant for substrate binding and specificity in choline oxidase. *Arch. Biochem. Biophys. 430*, 264–273.
58. Finnegan, S., Agniswamy, J., Weber, I. T., and Gadda, G. (2010) Role of Val464 in the flavin oxidation reaction catalyzed by choline oxidase. *Biochemistry 49*, 2952–2961.
59. Fraaije, M. W., and Mattevi, A. (2000) Flavoenzymes: diverse catalysts with recurrent features. *Trends Biochem. Sci. 25*, 126–132.
60. Pudek, M. R., and Bragg, P. D. (1976) Redox potentials of the cytochromes in the respiratory chain of aerobically grown *Escherichia coli*. *Arch. Biochem. Biophys. 174*, 546–552.